Eur. J. Mineral., 34, 375–383, 2022
https://doi.org/10.5194/ejm-34-375-2022

European Journal of Mineralogy
Open Access

Tomsquarryite, $NaMgAl_3(PO_4)_2(OH)_6 \cdot 8H_2O$, a new crandallite-derivative mineral from Tom's phosphate quarry, Kapunda, South Australia

Peter Elliott[1,2], **Ian E. Grey**[3], **William G. Mumme**[3], **Colin M. MacRae**[3], **and Anthony R. Kampf**[4]

[1]Department of Earth Sciences, School of Physical Sciences,
University of Adelaide, Adelaide 5005, South Australia, Australia
[2]South Australian Museum, North Terrace, Adelaide 5000, South Australia, Australia
[3]CSIRO Mineral Resources, Private Bag 10, Clayton South 3169, Victoria, Australia
[4]Mineral Sciences Department, Natural History Museum of Los Angeles County,
900 Exposition Boulevard, Los Angeles, CA 90007, USA

Correspondence: Ian E. Grey (ian.grey@csiro.au)

Received: 23 June 2022 – Accepted: 23 July 2022 – Published: 17 August 2022

Abstract. Tomsquarryite, $NaMgAl_3(PO_4)_2(OH)_6 \cdot 8H_2O$, is a new secondary phosphate mineral from Tom's phosphate quarry, Kapunda, South Australia. It occurs as colourless, talc-like hexagonal platelets, with diameters of a few tens of micrometres when formed from the decomposition of minyulite and as thicker ($\sim 10\,\mu m$) hexagonal crystals when formed from alteration of gordonite. Associated minerals are penriceite, elliottite, minyulite, angastonite and wavellite. The calculated density is $2.22\,g\,cm^{-3}$. Tomsquarryite crystals are uniaxial (+) with $\omega = 1.490(3)$, $\varepsilon = 1.497(3)$ (white light). Dispersion was not observed. The partial orientation is $Z \approx \boldsymbol{c}$. Electron microprobe analyses of the holotype specimen give the empirical formula $Na_{1.02}K_{0.02}Ca_{0.08}Mg_{1.26}Al_{2.86}(PO_4)_{2.00}(OH)_{3.82}F_{2.48} \cdot 7.70H_2O$, based on 22 anions. Tomsquarryite belongs to the trigonal crystal system, space group $R\bar{3}m$, with hexagonal unit-cell parameters $a = 6.9865(5)$ Å, $c = 30.634(3)$ Å and $V = 1294.9(4)$ Å^3 and with $Z = 3$. The crystal structure was refined using single-crystal diffraction data; $R_1 = 0.069$ for 303 reflections with $I > 2\sigma(I)$ to a resolution of 0.80 Å. The crystal structure is a derivative of the crandallite structure, with Ca^{2+} cations replaced by hydrated magnesium ions, $[Mg(H_2O)_6]^{2+}$, resulting in an expansion of the interlayer separation from 5.4 Å in crandallite to 10.2 Å in tomsquarryite. The results for tomsquarryite are compared with those for the chemically and structurally related minerals penriceite and elliottite.

1 Introduction

Secondary phosphate minerals form the most common chemical group of new species from Australian type localities. Of the 184 minerals first discovered and described from Australian localities since 1870, 57 species are phosphates (Sutherland et al., 2000; Elliott et al., 2013). The majority (30) derive from South Australian localities, of which the Kapunda–Angaston phosphate region (Fig. 1) is most prolific with seven type-locality minerals. The region includes the Klemm's (Moculta), St. John's, St. Kitt's and Tom's rock phosphate quarries, which have been mined intermittently for superphosphate production since the beginning of the 20th century, and the Penrice marble quarry, which contains phosphatic gossanous zones within the marble (Johns, 1976; Elliott et al., 2013). The Penrice quarry is the type locality for angastonite, $CaMgAl_2(PO_4)_2(OH)_4 \cdot 7H_2O$ (Mills et al., 2008; Grey et al., 2022a), and penriceite, $NaMgAl_3(PO_4)_2F_6 \cdot 9H_2O$ (Elliott et al., 2022), whereas Klemm's quarry is the type locality for aldermanite, $NaMgAl_3(PO_4)_2(OH)_6 \cdot 9H_2O$, the hydroxide analogue of penriceite (Harrowfield et al., 1981; Elliott et al., 2021).

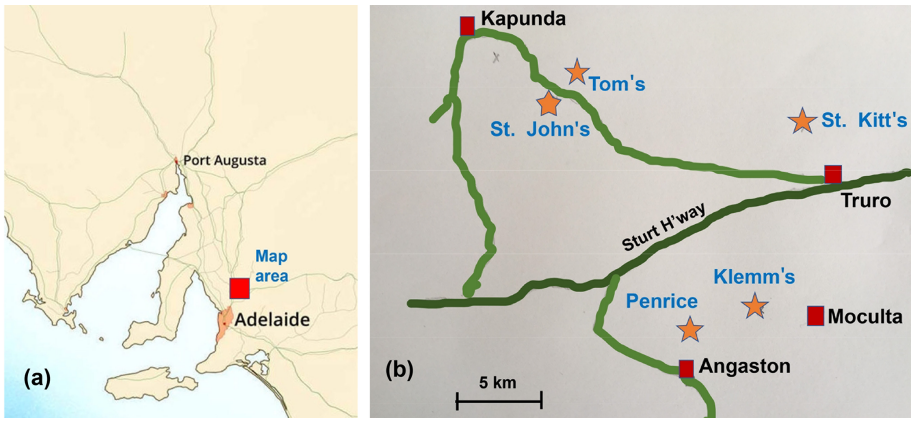

Figure 1. **(a)** Location of the Kapunda–Angaston phosphate province in a map of South Australia. **(b)** Phosphate deposits in the Kapunda–Angaston region.

Tom's quarry, located 5 km southeast of Kapunda (Fig. 1), is the only phosphate mine in the region that is still operating today. It is an open-cut mine that exploits phosphorite-type rock phosphate. The phosphorite is distributed through calcareous clay derived from the decomposition of argillaceous rocks underlying the Kapunda Marble formation (Elliott et al., 2013). To date, Tom's quarry has been the type locality for four secondary phosphate minerals. They are peisleyite, $Na_2Al_9[(P,S)O_4]_8(OH)_6 \cdot 28H_2O$ (Pilkington et al., 1982; Mills et al., 2011); kapundaite, $(Na,Ca)_2Fe_4^{3+}(PO_4)_4(OH)_3 \cdot 5H_2O$ (Mills et al., 2010); jahnsite-(CaFeMg), $CaFe^{2+}Mg_2Fe_2^{3+}(PO_4)_4(OH)_2 \cdot 8H_2O$ (Elliott, 2016); and elliottite, $NaMgAl_3(PO_4)_2F_6 \cdot 9H_2O$, a dimorph of penriceite (Grey et al., 2022b). We report here the characterisation of a fifth new secondary phosphate mineral from Tom's quarry, tomsquarryite, $NaMgAl_3(PO_4)_2(OH)_6 \cdot 8H_2O$. The new mineral and its name were approved by the International Mineralogical Association Commission on New Minerals, Nomenclature and Classification (IMA2022-018). Tomsquarryite is closely related, both compositionally and structurally, to aldermanite, penriceite and elliottite as will be discussed in this paper.

The name is for the location. The holotype and cotype specimens from Tom's quarry and the cotype from the Penrice marble quarry are housed in the mineralogical collections of the South Australian Museum, catalogue numbers G35033, G35034 and G35031, respectively.

2 Occurrence and paragenesis

Tomsquarryite was found in hand specimens collected by one of the authors (PE) in the mid 2000s at Tom's phosphate quarry, Kapunda, South Australia (34°21′ S, 138°55′ E) and in specimens collected by Vince Peisley in 1988–1989 at the Penrice marble quarry, located about 15 km southeast of Tom's quarry. In the specimens from both localities, thin layers of tomsquarryite and other intimately mixed fine-grained secondary phosphates coat a goethite-clay matrix (Tom's quarry) and a goethite, Mn oxide, muscovite matrix (Penrice quarry) (Fig. 2). Tomsquarryite is most commonly associated with angastonite (Grey et al., 2022a). Other closely associated minerals are penriceite (Elliott et al., 2022), elliottite (Grey et al., 2022b), minyulite and wavellite. The formation of tomsquarryite at the Penrice quarry is related to the alteration of minyulite, $KAl_2F(PO_4)_2 \cdot 4H_2O$, in a near-neutral solution (Grey et al., 2022c). K is leached, and the leach product takes up solution species Mg^{2+}, Ca^{2+} and Na^+ to form an amorphous phase that subsequently crystallises as tomsquarryite, elliottite and penriceite. At Tom's quarry, an alternative paragenesis was noted in South Australian Museum specimen G35033, involving progressive surface alteration of gordonite, $MgAl_2(PO_4)_2(OH)_2 \cdot 8H_2O$, most likely by a dissolution/reprecipitation mechanism in a Na- and F-bearing solution.

3 Description and experimental procedures

3.1 Appearance and properties

Tomsquarryite at the Penrice quarry occurs most commonly as talc-like platelets, with diameters of a few tens of micrometres and thicknesses of only $\sim 1\,\mu m$ (Fig. 3). At Tom's quarry, when formed from gordonite, it occurs as thicker ($\sim 10\,\mu m$) pseudohexagonal crystals flattened on {001} (Fig. 4). The crystals are colourless with a white streak. They exhibit the forms {001}, {100} and {110} and have perfect cleavage on {001}. The density was not measured due to paucity of material. The calculated density, based on the empirical formula for specimen G35033 and single-crystal unit-cell parameters, is $2.22\,g\,cm^{-3}$. Tomsquarryite crystals are uniaxial (+) with $\omega = 1.490(3)$ and $\varepsilon = 1.497(3)$ (white light). Dispersion was not observed. The partially determined

Figure 2. South Australian Museum specimen G35034. Field of view is 7 mm across. Photograph: Peter Elliott.

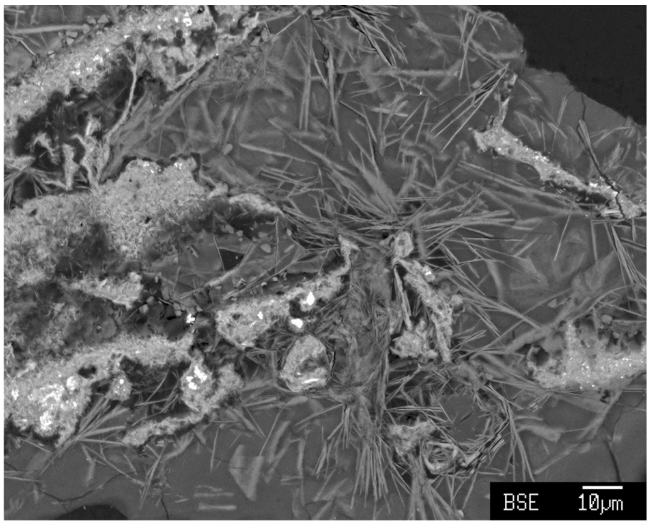

Figure 3. Backscattered electron image showing ultra-thin platelets of tomsquarryite in an amorphous CaMgAl phosphate matrix in Penrice quarry specimen G35031.

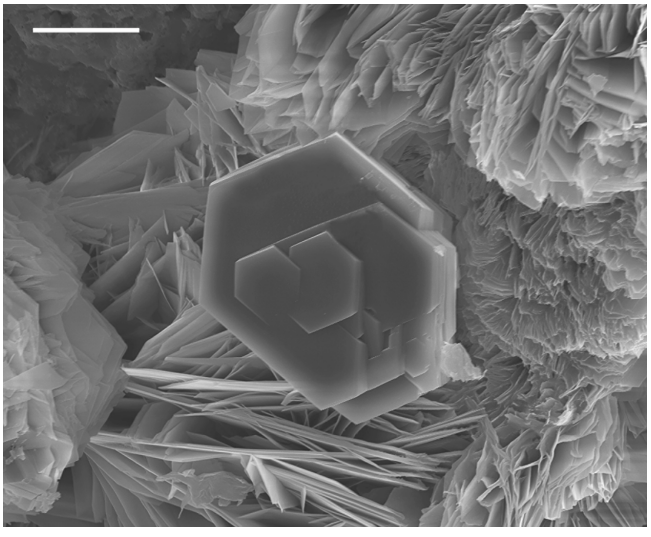

Figure 4. Scanning electron microscope image showing hexagonal crystals of tomsquarryite associated with penriceite in Tom's quarry specimen G35033. Scale bar is 10 µm.

orientation is $Z \approx \boldsymbol{c}$. Application of the Gladstone–Dale relationship (Mandarino, 1981) using the measured parameters for holotype specimen G35033 gives a compatibility index of 0.019 (superior).

3.2 Infrared spectroscopy

The infrared absorption spectrum of specimen G35031 of tomsquarryite (Fig. 5) was obtained on ground crystals using a Nicolet 5700 FTIR (Fourier-transform infrared) spectrometer (range 4000 to 700 cm^{-1}, transmission mode) equipped with a Nicolet Continuum IR microscope and a diamond-anvil cell. A broad band is observed in the OH-stretching region with a split maximum at 3240 and 3350 cm^{-1} and with shoulders at 3050 and 3600 cm^{-1}. The first three bands correspond to H-bonded O…O distances in the range 2.65 to 2.80 Å (Libowitzky, 1999), consistent with results from the crystal structure refinement. The band at 3600 cm^{-1} corresponds to very weak H bonding, also consistent with the structure determination. The H-O-H bending vibrations of H_2O are represented by a broad peak at 1650 cm^{-1}. By analogy with the IR spectrum for crandallite (Frost et al., 2011), with the same topology of PO_4 tetrahedra, the symmetric P-O stretching modes are represented by peaks at 1025 and 1045 cm^{-1} and a shoulder at 975 cm^{-1}, whereas shoulders at 1120 and 1180 cm^{-1} correspond to antisymmetric P-O stretching modes. A weak broad peak at 1450 cm^{-1} may correspond to carbonate impurity (Grey et al., 2011).

3.3 Chemical composition

Crystals of tomsquarryite from Tom's quarry (specimens G35033 and G35034) were analysed using wavelength-dispersive spectrometry on a JEOL JXA-8500F Hyperprobe operated at an accelerating voltage of 15 kV and a beam current of 2 nA. Aggregates of edge-on platelets were analysed, and the beam was defocused to 5 µm to minimise beam damage. Analytical results are given in Table 1. The H_2O content in Table 1 is based on the formula from the crystal structure refinement, $NaMgAl_3(PO_4)_2X_6 \cdot 8H_2O$, with X equal to F and OH. The quantification was applied using the library of Stratagem®, a commercial software based on the work of Pouchou and Pichoir (1991, 1993). The H_2O was included in the matrix correction. For comparison, the analyses of tomsquarryite from the Penrice marble quarry (specimen G35031) are also given in Table 1. As shown in Fig. 3, the crystals in this specimen were ultra-thin, talc-like platelets in an amorphous matrix, and low analysis totals

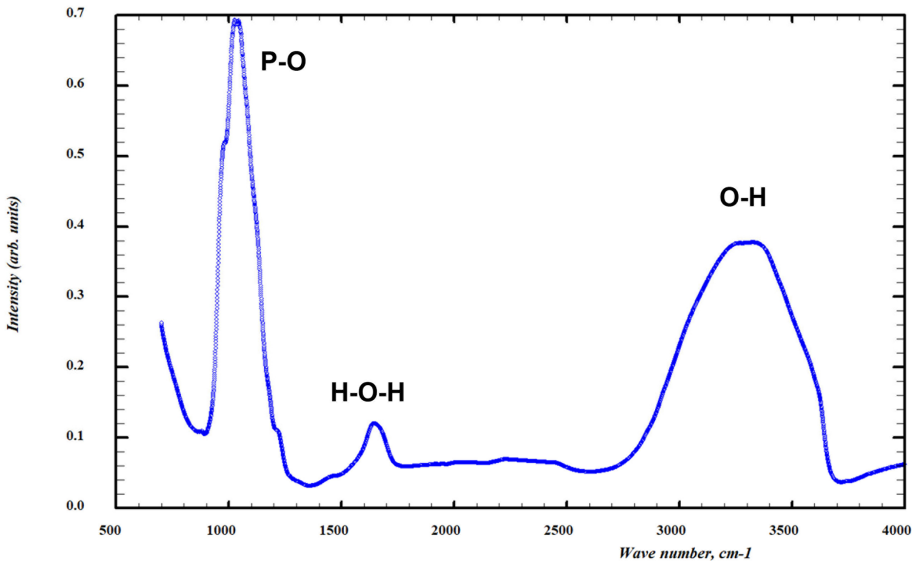

Figure 5. Infrared spectrum for tomsquarryite.

were obtained. The analyses were scaled to give a total of 100 % for the calculation of the empirical formula.

Empirical formulae, normalised to 22 anions, are the following.

G35033: $Na_{1.02}K_{0.02}Ca_{0.08}Mg_{1.26}Al_{2.86}(PO_4)_{2.00}(OH)_{3.82}F_{2.48} \cdot 7.70H_2O$

G35034: $Na_{0.98}K_{0.02}Ca_{0.07}Mg_{0.97}Al_{2.89}(PO_4)_{2.16}(OH)_{2.88}F_{2.41} \cdot 8.07H_2O$

G35031: $Na_{0.73}K_{0.01}Ca_{0.24}Mg_{1.30}Al_{2.83}(PO_4)_{1.98}(OH)_{3.73}F_{2.64} \cdot 7.71H_2O$

The simplified formula is (Na, Ca, K)Mg(Al, Mg)$_3$(PO$_4$)$_2$(OH,F)$_6 \cdot 8H_2O$.

The ideal endmember formula is $NaMgAl_3(PO_4)_2(OH)_6 \cdot 8H_2O$, which requires Na_2O 5.49, MgO 7.14, Al_2O_3 27.10, P_2O_5 25.15 and H_2O 35.12, totalling 100 wt %.

3.4 Powder X-ray diffraction

Powder X-ray diffraction (PXRD) data were collected on ground samples of Penrice specimen G35031 and Tom's quarry specimen G35033. The patterns were obtained at room temperature using a Panalytical Aeris diffractometer employing Co$K\alpha$ radiation. Step-scan data were collected in the 2-theta range 5 to 80° using a step size of 0.022°. Tomsquarryite was the major phase in the PXRD of G35031 together with minor quartz, wavellite and penriceite, whereas the PXRD for G35033 contained tomsquarryite and penriceite as co-majors. Refinement of the PXRD data using FullProf (Rodriguez-Carvajal, 1990) gave the following hexagonal cell parameters.

G35031: $a = 6.9967(5)$ Å, $c = 30.711(3)$ Å, $V = 1302.0(3)$ Å^3

G35033: $a = 6.988(2)$ Å, $c = 30.796(7)$ Å, $V = 1302(1)$ Å^3

Observed and calculated d values, intensities and indices for G35031 are given in Table 2.

3.5 Single-crystal structure analysis

Crystals of tomsquarryite are usually minute talc-like platelets with thicknesses of ∼ 1 µm that are unsuitable for single-crystal (SC) diffraction data collections. The specimen G35033, however, contains platelets that are typically 10 µm thick (Fig. 4), and they give sharp diffraction spots. A crystal with dimensions 0.055 × 0.055 × 0.010 mm was mounted for a data collection using an Oxford Diffraction Xcalibur E diffractometer equipped with a EOS (electro-optical system) CCD (charge-coupled device) detector. An ω scan was used to collect intensity data at room temperature using Mo$K\alpha$ radiation ($\lambda = 0.71073$ Å). The diffraction data displayed trigonal symmetry, with possible space groups R–3m (no. 166) or its non-centrosymmetric subgroups. Refined unit-cell parameters from the SC data are $a = 6.9865(5)$ Å, $c = 30.634(3)$ Å and $V = 1294.9(4)$ Å^3.

A structure solution for tomsquarryite in space group R–3m was obtained using SHELXT (Sheldrick, 2015). The solution had one Al, one P and three O sites that formed a crandallite-type layer (Blount, 1974), together with a Na atom at the centre of the hexagonal rings in the crandallite layers, and a Mg atom in the interlayer region at (0, 0, 1/2). Difference Fourier maps gave three partially occupied anion sites with distances to Mg in the range 2.02 to 2.15 Å and an anion site that completed eight coordination to Na. SHELXL refinement (Sheldrick, 2015) with anisotropic displacement parameters for the metal atoms and with refinement of the

Table 1. Electron microprobe analyses, with standard deviations in brackets.

	G45033 Tom's quarry		G35034 Tom's quarry	G35031 Penrice	
	Mean of 8	Range	Mean of 15	Mean of 2	
Na_2O	5.46 (0.33)	4.74–6.36	5.30 (0.46)	3.51	Albite
K_2O	0.16 (0.12)	0.05–0.34	0.19 (0.27)	0.05	Adularia
CaO	0.77 (0.33)	0.41–1.15	0.69 (0.35)	2.11	Apatite
MgO	8.80 (0.56)	7.85–9.29	6.83 (0.31)	8.18	Spinel
Al_2O_3	25.3 (1.3)	23.4–26.8	25.8 (0.8)	22.4	Berlinite
P_2O_5	24.6 (1.8)	22.0–26.4	26.8 (1.8)	21.8	Berlinite
F	8.16 (0.80)	6.95–9.06	8.02 (0.78)	7.78	CaF_2
-O=F	−3.44		−3.38	−3.28	
H_2O	30.0		30.0	30.0	
Total	99.81		100.25	92.55	

Table 2. Powder X-ray diffraction data (d in Å) for tomsquarryite.

I_{obs}	d_{meas}	d_{calc}	h	k	l
100	10.24	10.24	0	0	3
34	5.944	5.945	1	0	1
32	5.643	5.636	0	1	2
19	5.119	5.118	0	0	6
23	4.755	4.756	1	0	4
10	4.312	4.314	0	1	5
34	3.499	3.498	1	1	0
17	3.239	3.243	0	1	8
26	3.015	3.015	0	2	1
33	2.888	2.888	1	1	6
23	2.818	2.818	0	2	4
16	2.557	2.559	0	0	12
11	2.200	2.201	1	0	13
		2.194	2	1	4
6	2.064	2.065	1	1	12
		2.063	0	1	14
7	1.982	1.982	0	3	3
5	1.967	1.967	1	2	8
9	1.879	1.879	0	3	6
24	1.749	1.749	2	2	0
9	1.620	1.621	0	2	16
5	1.444	1.444	2	2	12

occupancies of the anions in the partially occupied sites converged at $R_1 = 0.069$ for 303 independent reflections with $I > 2\sigma(I)$ to a resolution of 0.80 Å. Further details of the data collection and refinement are given in Table 3. The refined atom coordinates, equivalent isotropic displacement parameters and calculated bond valence sums (BVSs, Gagné and Hawthorne, 2015) are reported in Table 4, and polyhedral bond distances and likely H-bonded O-O pairs are given in Table 5.

4 Discussion

A projection of the crystal structure of tomsquarryite along [110] is shown in Fig. 6a. It is essentially the same as the structure of crandallite but with a hydrated magnesium ion, $[Mg(H_2O)_6]^{2+}$, replacing Ca in the interlayer, resulting in an increase in the interlayer separation from 5.4 Å in crandallite to 10.2 Å in tomsquarryite. The tomsquarryite structure also differs from that for crandallite in having a sodium cation at the centre of the hexagonal rings in the heteropolyhedral layers. The sodium coordinates to six intralayer OH/F anions and to two H_2O (Ow4) perpendicular to the layer, giving eight coordination in the form of a scalenohedron. The same Na coordination occurs in penriceite (Elliott et al., 2022). The mean Mg-O distance is 2.09 Å, and the ratio of the summed site occupancies of the coordinating Ow1 to Ow3 atoms to that for Mg is 6.06; both being consistent with octahedral coordination for Mg. The octahedra display severe rotational disorder about [001]. Due to disordered, partially occupied Ow sites and the replacement of OH by F, the H atoms could not be unambiguously located in the refinement. The BVSs in Table 4 correspond to OH/F at the O3 site and H_2O at the Ow sites. The O1 site, with a low BVS of 1.34, receives strong H bonds from both Ow2 and Ow3 (Table 5). The BVS values for the Na (1.18) and Al (2.89) sites are consistent with minor substitution of Ca and Mg, respectively, at these sites.

Table 3. Crystal data and structure refinement for tomsquarryite.

Formula	$NaMgAl_3(PO_4)_2(OH)_6 \cdot 8H_2O$
Formula weight	570.2
Temperature	293 K
Wavelength	0.71073 Å
Space group	$R\text{–}3m$
Unit-cell dimensions	$a = 6.9864(5)$ Å
	$c = 30.634(3)$ Å
Volume	1294.9(2) Å^3
Absorption correction	Empirical multi-scan
Crystal size	$0.055 \times 0.055 \times 0.010$ mm
Theta range for data collection	3.43 to 26.34°.
Index ranges	$-8 \Leftarrow h \Leftarrow 8, -8 \Leftarrow k \Leftarrow 8, -37 \Leftarrow l \Leftarrow 37$
Reflections collected	14 248
Independent reflections/R(int)	375/0.20
Reflections with $I_o > 2\sigma(I)$	303
Refinement method	Full-matrix least-squares on F^2
Data/restraints/parameters	375/0/33
Goodness-of-fit	1.10
Final R indices [$I > 2\sigma(I)$]	$R_1 = 0.069$, w$R(F^2) = 0.163$
R indices (all data)	$R_1 = 0.085$, w$R(F^2) = 0.172$

Table 4. Atom coordinates for tomsquarryite.

	Site	Occ.	x	y	Z	Ueq, Å^2	BVSs
Na	3*a*	1	0	0	0	0.039(2)	1.18
Mg	3*b*	1	0	0	1/2	0.024(2)	2.09
Al	9*e*	1	1/2	0	0	0.007(1)	2.89
P	6*c*	1	0	0	0.2570(1)	0.010(1)	5.01
O1	6*c*	1	0	0	0.2078(3)	0.021(2)	1.34
O2	18*h*	1	0.7859(4)	0.2141(4)	0.6083(1)	0.012(1)	1.76
O3	18*h*	1	0.5382(4)	0.4617(4)	0.6811(1)	0.006(1)	1.05
Ow1	18*h*	0.336(16)	0.940(1)	0.060(1)	0.4382(6)	0.034(4)	0.39
Ow2	18*h*	0.204(26)	0.163(3)	0.837(3)	0.514(1)	0.034(4)	0.39
Ow3	36*i*	0.235(15)	0.329(4)	0.254(4)	0.4840(7)	0.034(4)	0.29
Ow4	6*c*	1	0	0	0.0796(5)	0.066(4)	0.34

Table 5. Polyhedral bond lengths [Å] and likely H-bonded anions in tomsquarryite.

Al-O2 ×2	1.878(5)	Na-O3 ×6	2.519(5)
Al-O3 ×4	1.882(2)	Na-Ow4 ×2	2.439(15)
Av.	1.881	Av.	2.499
P-O1	1.507(10)	Mg-Ow1 ×6	2.030(17)
P-O2 ×3	1.544(5)	Mg-Ow2 ×6	2.02(4)
Av.	1.535	Mg-Ow3 ×12	2.15(2)
		Av.	2.09
Ow1-O2	2.72	Ow3-O1	2.76
Ow1-O3	2.89	Ow3-O1	2.97
Ow2-O1	2.67	Ow3-Ow4	3.05
Ow2-O4	3.03	Ow4-O3	3.18

Table 6. Comparison of properties for tomsquarryite, elliottite and penriceite.

	Tomsquarryite	Elliottite	Penriceite
Endmember formula	$NaMgAl_3(PO_4)_2(OH)_6 \cdot 8H_2O$	$NaMgAl_3(PO_4)_2F_6 \cdot 9H_2O$	$NaMgAl_3(PO_4)_2F_6 \cdot 9H_2O$
Symmetry	Trigonal, *R*-3*m*	Monoclinic, *C*2/*m*	Monoclinic, $P2_1/c$
a (Å)	6.9865(5)	12.2420(10)	13.478(3)
b (Å)		7.0118(7)	9.971(2)
c (Å)	30.634(3)	11.2946(9)	6.9990(10)
β (°)		101.19(1)	97.20(3)
Volume (Å^3), *Z*	1294.9(4), 3	951.1(2), 2	933.2(3), 2
Optics	Uniaxial (+), $\omega = 1.490(3)$. $\varepsilon = 1.497$	Biaxial (+) $\alpha = \beta = 1.475(2)$, $\gamma = 1.479(2)$, $2V(\text{calc}) = 0°$	Biaxial (+), $\alpha = 1.502(2)$, $\beta = 1.503(2)$, $\gamma =$ n.d.
Strongest lines	10.24, 100 (003)	11.08, 100 (001)	13.39, 100 (100)
In PXRD	5.945, 34 (101)	6.059, 9 (110)	8.000, 30 (110)
d, *I*, (*hkl*)	5.643, 32 (012)	5.782, 12 (−201)	5.562, 26 (210)
	3.499, 34 (110)	5.106, 31 (111)	5.718, 12 (011)
	3.015, 26 (021)	2.882, 8 (−402)_	2.855, 16 (022)
	2.888, 33 (116)	2.852, 17 (221)	2.782, 15 (420)

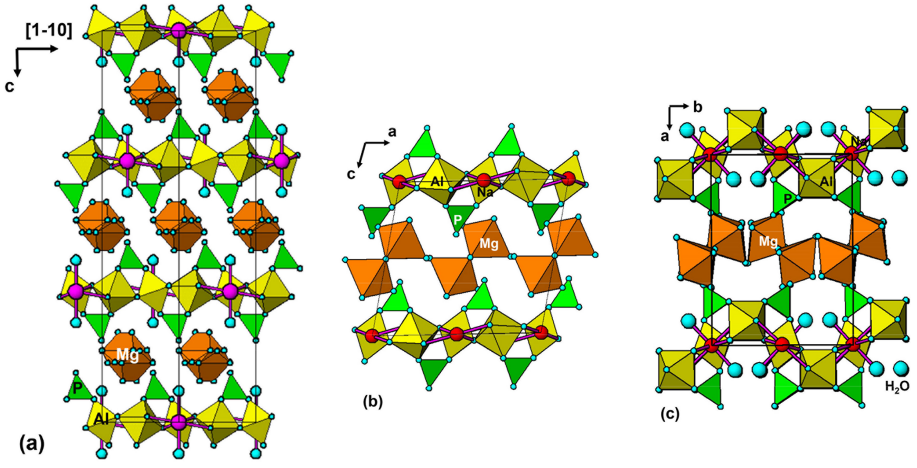

Figure 6. **(a)** Projection of tomsquarryite structure along [110]. **(b)** [010] projection of the structure of elliottite. **(c)** [001] projection of the structure of penriceite.

Tomsquarryite is closely related, both compositionally and structurally, to elliottite, $NaMgAl_3(PO_4)_2F_6 \cdot 9H_2O$ (Grey et al., 2022b). The structure of elliottite is shown in projection along [010] in Fig. 6b. Both have crandallite-derivative layer structures, which are built from planer nets of trans-corner-shared Al-centred octahedra, decorated with PO_4 tetrahedra. In tomsquarryite, Na atoms at the centres of the six-member rings have eight-coordinated scalenohedral coordination, whereas in elliottite, the Na is six-coordinated as a very flat octahedron with the next-nearest anions being over 3 Å away. In tomsquarryite, the interlayer $Mg(H_2O)_6$ octahedra are isolated, whereas in elliottite they share edges, giving half-occupied $Mg_2(H_2O)_{10}$ dimers. Elliottite has a larger

layer spacing, 11.0 Å, and accommodates extra H_2O in the interlayer region.

Tomsquarryite is also chemically and structurally related to penriceite, $NaMgAl_3(PO_4)_2F_6 \cdot 9H_2O$ (Elliott et al., 2022). Whereas in tomsquarryite the heteropolyhedral layers are built from planar nets of trans-corner-shared Al-centred octahedra, the layers in penriceite and the isostructural mineral aldermanite (Elliott et al., 2021) have a sawtooth shape and involve both trans- and cis-corner-sharing of octahedra, shown in Fig. 6c. The layers in penriceite can be described in terms of periodic unit-cell-scale twinning of the crandallite-type layers in tomsquarryite (and elliottite). The relationship between the two structures is similar to that between the structures of orthoenstatite and clinoenstatite, for which the orthorhombic orthoenstatite structure has been described as unit-cell twinning of the monoclinic clinoenstatite structure (Morimoto and Koto, 1969). Penriceite has a much larger layer spacing (13.5 Å), resulting in a PXRD pattern very different from those of tomsquarryite (with a 10.2 Å layer spacing) and elliottite (with an 11.0 Å layer spacing). The properties of tomsquarryite, elliottite and penriceite are compared in Table 6.

Data availability. Crystallographic data for tomsquarryite are available in the Supplement.

Supplement. The supplement related to this article is available online at: https://doi.org/10.5194/ejm-34-375-2022-supplement.

Author contributions. IEG oversaw the research and wrote the manuscript. PE supplied the specimens and images and collected the X-ray diffraction data and infrared spectrum. WGM assisted in the data processing. CMM conducted the microprobe analyses. ARK measured the optical properties.

Competing interests. The contact author has declared that none of the authors has any competing interests.

Disclaimer. Publisher's note: Copernicus Publications remains neutral with regard to jurisdictional claims in published maps and institutional affiliations.

Acknowledgements. The authors thank Cameron Davidson and Matthew Glenn for help with electron microprobe (EMP) sample preparation and scanning electron microscope (SEM) studies. The infrared spectrum was acquired with the assistance of the Forensic Science Centre, Adelaide. We thank the Bragg Crystallography Facility, University of Adelaide, for use of their single-crystal diffractometer.

Review statement. This paper was edited by Sergey Krivovichev and reviewed by Alan Pring and one anonymous referee.

References

Blount, A. M.: The crystal structure of crandallite, Am. Mineral., 59, 41–47, 1974.

Elliott, P.: Jahnsite-(CaFeMg), a new mineral from Tom's quarry, South Australia: description and crystal structure, Eur. J. Mineral., 28, 991–996, https://doi.org/10.1127/ejm/2016/0028-2562, 2016.

Elliott, P., Peisley, V., and Mills, S. J.: The phosphate deposits of South Australia, Aust. J. Mineral., 17, 3–32, 2013.

Elliott, P., Grey, I. E., and Willis, A. C.: Redefinition of the formula for aldermanite, $[Mg(H_2O)_6][Na(H_2O)_2Al_3(PO_4)_2(OH,F)_6] \cdot H_2O$, and its crystal structure, Mineral. Mag., 85, 348–353, 2021.

Elliott, P., Grey, I. E., MacRae, C. M., Kampf, A. R., and Davidson, C.: Penriceite, $[Mg(H_2O)_6][Na(H_2O)_2Al_3(PO_4)_2F_6] \cdot H_2O$, the F-analogue of aldermanite, from the Penrice marble quarry, South Australia, Aust. J. Mineral., 23, 6–12, 2022.

Frost, R., Xi, Y., Palmer, S., and Pogson, R.: Vibrational spectroscopic analysis of the mineral crandallite $CaAl_3(PO_4)_2(OH)_5.(H_2O)$ from the Jenolan caves, Australia, Spectrochim. Acta A, 82, 461–466, 2011.

Gagné, O. C. and Hawthorne, F. C.: Comprehensive derivation of bond-valence parameters for ion pairs involving oxygen, Acta Crystallogr. B, 71, 562–578, 2015.

Grey, I. E., Shanks, F. L., Wilson, N. C., Mumme, W. G., and Birch, W. D.: Carbon incorporation in plumbogummite-group minerals, Mineral. Mag., 75, 145–158, 2011.

Grey, I. E., Elliott, P., Mumme, W. G., MacRae, C. M., Kampf, A. R., and Mills, S. J.: Redefinition of angastonite, $CaMgAl_2(PO_4)_2(OH)_4 \cdot 7H_2O$, as an amorphous mineral, Eur. J. Mineral., 34, 215–221, https://doi.org/10.5194/ejm-34-215-2022, 2022a.

Grey, I. E., Mumme, W. G., MacRae, C. M., Kampf, A. R., and Mills, S.J.: Elliottite, $NaMgAl_3(PO_4)_2F_6 \cdot 9H_2O$; a new crandallite-derivative mineral from Tom's phosphate quarry, Kapunda, South Australia, Aust. J. Mineral., 23, 13–20, 2022b.

Grey, I. E., MacRae, C. M., Elliott, P., Mills, S. J., and Downes, P. J.: Minyulite, $KAl_2F(PO_4)_2 \cdot 4H_2O$. Approval of revised formula and its stability in South Australian rock phosphate deposits, Aust. J. Mineral., 23, 21–25, 2022c.

Harrowfield, I. R., Segnit, E. R., and Watts, J. A.: Aldermanite, a new magnesium aluminium phosphate, Mineral. Mag., 44, 59–62, 1981.

Johns, R. K.: Phosphate, South Australia, in: Economic geology of Australia and Papua New Guinea, 4, Industrial minerals and rocks, edited by: Knight, C. L., 282–285, Australasian Institute of Mining and Metallurgy, Monograph Series no. 8, ISBN 0909520224, 1976.

Libowitzky, E.: Correlation of O-H stretching frequencies and O-H. . . O hydrogen bond lengths in minerals, Monatsh. Chem., 130, 1047–1059, 1999.

Mandarino, J. A.: The Gladstone-Dale relationship: Part IV. The compatibility concept and its application, Can. Mineral., 19, 441–450, 1981.

Mills, S. J., Groat, L. A., Wilson, S. A., Birch, W. D., Whitfield, P. S., and Raudsep, M.: Angastonite, $CaMgAl_2(PO_4)_2(OH)_4 \cdot 7H_2O$: a new phosphate mineral from Angaston, South Australia, Mineral. Mag., 72, 1011–1020, 2008.

Mills, S. J., Birch, W. D., Kampf, A. R., Christy, A. G., Pluth, J. J., Pring, A., Raudsepp, M., and Chen, Y.-S.: Kapundaite, a new phosphate species from Tom's quarry, South Australia: description and structural relationship to melonjosephite, Am. Mineral., 95, 754–760, 2010.

Mills, S. J., Ma, C., and Birch, W. D.: A contribution to understanding the complex nature of peisleyite, Mineral. Mag., 75, 2733–2737, 2011.

Morimoto, N. and Koto, K.: The crystal structure of orthoenstatite, Z. Kristallogr., 129, 65–83, 1969.

Pilkington, E. S., Segnit, E. R., and Watts, J. A.: Peisleyite, a new sodium aluminium sulphate phosphate, Mineral. Mag., 46, 449–452, 1982.

Pouchou, J.-L. and Pichoir, F.: Quantitative analysis of homogeneous or stratified microvolumes applying the model PAP, in: Electron Probe Quantitation, edited by: Heinrich, K. F. J. and Newbury, D. E., Plenum Press, New York, 31–75, ISBN 978-1-4899-2617-3, 1991.

Pouchou, J.-L. and Pichoir, F.: Electron probe X-ray microanalysis applied to thin surface films and stratified specimens, Scanning Microscopy Suppl., 7, 167–189, 1993.

Rodriguez-Carvajal, J.: FULLPROF: A Program for Rietveld refinement and Pattern Matching Analysis: Satellite meeting on powder diffraction of the Fifteenth General Assembly and International Congress of Crystallography, 16–19 July 1990, Toulouse, France, 1990.

Sheldrick, G. M.: Crystal-structure refinement with SHELX, Acta Crystallogr. C, 71, 3–8, 2015.

Sutherland, F. L., Pogson, R. E., Birch, W. D., Henry, D. A., Pring, A., Bevan, A. W. R., Stalder, H. A., and Graham, I. T.: Mineral species first described from Australia and their type specimens, Aust. J. Mineral., 6, 105–128, 2000.